THE INFLUENCE OF MICROSTRUCTURE AND GEOMETRIC FACTORS ON THE STRESS STATE AND THE FRACTURE TOUGHNESS OF CERAMICS

F. E. Buresch
Institute for Reactor Materials, Nuclear Research Center Jülich GmbH,
P.O. Box 1913, D-5170 Jülich
Federal Republic of Germany

ABSTRACT

The toughness of ceramics is controlled by micromechanical features which occur by microcracking in the process zone during stress redistribution. The size of the process zone is determined by microstructural parameters, especially the specific fracture energy, and inversely proportional to the Weibull-modulus, and lies for many fine-grained and coarse-grained ceramics in the range of 0.1 to 1 mm.

Toughness of ceramics increases with notch radius for $\rho > \rho_c$. This dependence, however, is influenced by the microstructure as well as the specimen or component geometry. Concerning materials with high specific fracture energy it is possible to indicate a material-specific K_{Ic}-value independent of the specimen size, if certain geometric conditions with regard to notch and sample geometry are fulfilled. This corresponds to plane strain including near crack tip plasticity.

Materials with low specific fracture energy like graphite or refractories cause remote microcracking specially if specimens with large notch root radii are used, corresponding to remote plasticity of any metals. It is possible that these materials bring out a "plastic hinge" in bent specimen. The K_I-value of these ceramics depends on specimen size. This corresponds to plane stress.

KEYWORDS

Toughness; near crack tip/remote plasticity; stress state; fracture mechanism (materials); crack propagation; size of process zone; microstructure; microcrack density distribution; photoelasticity; ceramics.

1. INTRODUCTION AND PURPOSE OF THE INVESTIGATION

Evaluating mechanical properties of ceramic materials, one usually starts from the fact that they are "brittle". According to the present understanding, a brittle crack occurs without significant energy dissipation in a highly stressed volume. With that assumption it were unnecessary to consider for ceramics the influence of "plastified volume regions" on fracture-mechanic parameters, determined on small specimens, as well as the influence on the dimensioning of tension-loaded

ceramic components, as used for gasturbines, HTRs or plant equipment, which is significant for metallic materials.

Recent theoretical and experimental investigations show, however, that ceramic materials break by a coagulation of microcracks, after they have accumulated to a critical density in inhomogeneously stressed volume regions /1/. Energy is dissipated with the formation and growing of microcracks. The criterion of the critical microcrack density then is equivalent to a critical energy dissipation and thereby to the energy density criterion of the process zone /2/, if the increased compliance of the material caused by microcracks in a discrete volume region can be associated with a reduced Young's modulus. Thus, as in the case of metals, very high stresses on notches and cracks cause plasticities in near crack tip or even remote areas. These plasticities, along with geometric factors of specimens and components, determine the respective stress state and thereby the significance of the mechanical characteristic values entering the calculations.

Rules established in earlier studies /3-8/ will be completed in the following to evaluate fracture-mechanic values determined on small specimens and for its transferability to components, each for a material with low and high energy dissipation. The first group involves fine-grained ceramics like alumina and silicon carbide as applied, for example, as cutting tool and for structural materials of gas-turbines. Examples are quoted of fracture mechanical investigations on eight fine-grained Al_2O_3-grades /3-7/. The second group involves coarse-grained ceramic products like refractories, also including coarse-grained graphites; fracture-mechanic investigations of a reactor graphite are quoted /7,8/.

For these two groups of materials, characteristic values of constitutive equations and the respective regions of validity are given. The determining parameters are geometric factors and the degree of plasticity, respectively. An essential parameter for microcrack plasticity is the energy for the intergranular and transgranular specific fracture energy γ_S or the grain boundary energy, respectively. γ_S is "high" in the first of the mentioned material groups ($\sim$ 1 J/m^2), and "low" in the second one ($\sim$ 0.1 J/m^2).

2. MATERIAL PARAMETERS AND MICROCRACKING

2.1 Material-specific and Geometric Parameters of Microcracking

The plasticity by microcracking of ceramics effects a stress redistribution mechanically highly stressed volume regions. The kind and extent of stress redistribution is determined by length, density, orientation as well as by elastic interaction of microcracks. The mechanisms for the nucleation and growth of microcracks are given by the lattice structure of the participating phases and the microstructure of the material. Of particular importance is the energy of the specific intergranular and transgranular fracture energy and the grain and pore size distribution.

The geometric factors are the dimensions of specimens, components and notches with regard to a characteristic size given by the microstructure, for which the average grain size is taken.

2.2 Distribution of Length and Density of Microcracking

The volume dependence of the average fracture strength, especially with regard to high specific fracture energy, is based on the distribution of material defects. In general these defects are inhomogeneities like micropores, microcrack

nucleation sites as a consequence of residual stresses of 2nd and 3rd order, or microstructural notches of different stress concentration, or microcracks of different lengths. These defects are statistically distributed over the volume of a component or over many specimens taken from one batch, according to an asymptotic extreme value function. The failure of a component (specimen) occurs, if one single volume element breaks due to the critical crack length a_c at the critical strength σ_c. The Cauchy distribution introduced by Frêchet has generally proved in literature to be a good approximation for the analytic representation of the distribution of microcracks of critical length in a volume element /9/.

This function

$$P_a(a_c) = \exp - \left(\frac{a_c}{a_n}\right)^{-\alpha} \tag{1}$$

is limited for $a_c \to \infty$ by one, and for $a_c \to 0$ by zero. The microcrack length a_n is associated in the following with a "standard" value.

Using the Griffith relation for unimodal defect systems, i.e. for an isotropic and homogeneous material with $K_{Ic}(a_c) = K_{Ic}(a_n)$ /4/

$$K_{Ic} = \sigma_c \sqrt{\pi a_c} \tag{2}$$

the distribution of defects in eq. (1) can be associated with a distribution of critical strength

$$P(\sigma) = 1 - \exp - \left(\frac{\sigma_c}{\sigma_n}\right)^m \tag{3}$$

This means that each defect distribution is functionally associated with a constitutive equation, in general by $\sigma = \varepsilon E$, with $E = f(P^+)$. P^+ is the porosity which has to be constant for a specific distribution.

According to the rules of probability calculus, we then receive for a volume consisting of many elements

$$P(\sigma) = 1 - \exp - \sum_{i=1} \frac{V_i}{V_o} \left(\frac{\sigma_o}{\sigma_n}\right)^m \tag{4}$$

The fracture stresses will be ordered according to the specific microstructure in the "Weibull-diagram" by the equations (3) and (4), where the distribution parameter of the defects m is measured in the known fashion, $n(\sigma) = (\sigma_c/\sigma_n)^m$ is a measure for the number of critical microcracks in the volume element /7,10/. Then $n(\sigma)/V_o$ is the density of these microcracks referred to the volume unit V_o. The microcracking density is small in general. Then, according to eq. (4),

$$\frac{ß}{ß_o} = 1 - \exp - n\,(\sigma)^m \tag{5}$$

is a measure for the distribution function of the microcrack density, referred to microcrack nucleation sites $ß_o$ /7/.

2.3 Distributions of Microcrack Length and Grain Sizes

As was shown in earlier studies /4-6/, microcracks mainly originate from residual stresses of 2nd order, which find their origin in the anisotropy of physical con-

stants of crystallites (grains), e.g. the anisotropy of linear thermal expansion or by phase transformations /11, 23/. Residual stresses on the basis of an anisotropy of the thermal expansion coefficients $\Delta\alpha$ with residual strains $= \Delta\alpha\ \Delta T$ during cooling-down to room temperature (ΔT) beyond a critical temperature after sintering can be associated with a microscopic energy release rate of /4,14/

$$g_{IE} = \frac{E\varepsilon^2}{6\pi(1-\nu^2)^2}\, d = \frac{k_{IE}^2}{E} \qquad (6)$$

which increases linearly with grain size. A microcrack occurs spontaneously, e.g. with cooling down from sintering temperature /12-15/ or by superposing external stresses or residual stresses of 1st order corresponding to an extreme value criterion /14/, if the fracture energy release rate from external stresses $G_{Ic} \geq G_I$ and the fracture energy rate G_{Io} without residual stresses depending upon the load history obeys the relation

$$G_{Ic} \geq G_I = G_{Io} - g_{IE} \qquad (7)$$

For the first critical microcrack, G_{Io} corresponds to the intergranular or transgranular specific fracture energy γ_s, which according to the material is of the order of 0.1 ... 1 J/m^2. With increasing stress intensity, the right hand side of eq. (7), with increasing microcrack density - corresponding to the "avalanche effect" in acoustic emission analysis -, changes into the value of critical fracture energy release rate G_{Ic} (see also /1/).

It was observed that the length of microcracks caused by residual stresses, corresponding to the energy density of residual stresses (see eq. (6), is of the order of magnitude of the corresponding grain sizes /14/. Fréchet's defect distribution of eq. (1) thus can be associated with a grain size distribution. This means, this distribution approximates a "log-normal distribution" of grain sizes, which is often found for fine-grained ceramics. The "log-normal distribution" of grain sizes then corresponds according to equations (1) and (6) to a "log-normal distribution" of stress intensity factors of microcracks of the critical length $a_c = f(k_{IE})$.

2.4 The Influence of the Distribution of Length of Microcracks on the Size of the Process Zone

In plane strain and small microcrack plasticity (corresponding to small scale yielding), ρ_c is an autonomous area. It is independent of geometric parameters of the specimen, or of a component, as well as of external forces /16/. The autonomy condition is fulfilled, if ρ_c is small with respect to dimensions of specimens and components. However, ρ_c cannot be infinitely small, because the region of microcracking involves an elastic continuum. ρ_c thus has to be larger than the dimensions of the structure parameters grain size and pore size, which characterize the inhomogeneity of a material. This means, however, ρ_c is large with regard to the notch root radius and, on the other hand, small compared to specimen dimensions.

The nucleation and growth of microcracks within ρ_c is a statistical process, which depends on the distribution of defects or grain size (eq. (1) and (6)) of a material /10,17/. For the distribution of the microcrack density at a distance r from the crack tip for a unimodal defect system, it was found /7/

$$\frac{\beta}{\beta_o} = 1 - \exp - \left(\frac{K_{Ic}}{k_{Ic}}\right)^m \left(\frac{r}{a_m}\right)^{-\frac{m}{2}} \qquad (8)$$

The size of the process zone thus is determined by the number of microcracks in the volume element $n(\sigma)$ and the distribution parameter m. $k_{Ic} = \sqrt{2\,\gamma_s E} = \sqrt{\gamma_s E}$ is the local threshold value (standard value) of the stress intensity for one microcrack. Taking into account the simplifications made for equations (1,3-5) (see also /7/), the size of the process zone referred to the length of a microcrack is with $r = \rho_c$ given by

$$\frac{\rho_c}{a_m} = \exp\left(\ln \frac{G_{Ic}}{2\gamma_s} + \frac{B^+}{m}\right) \qquad (9)$$

Figure 1 shows curves of the above equation for different values of $n = \sqrt{G_{Ic}/2\gamma_s}$ and m. a_m is the length of a microcrack. The decrease of ρ_c with increasing Weibull-modulus m is physically reasonable and has been confirmed experimentally /4,5/.

Thus the microcrack density decreases steeply close to a notch. The size of the process zone, in accordance with physical reasons, is influenced by the microscopic specific fracture energy $2\,\gamma_s$ for the formation of microcracks, eqs. (1) and (6), as well as by the distribution parameter m of the defects. For an ideal linear-elastic homogeneous and isotropic material is $K_{Ic} = k_{Ic}$ and $m \to \infty$; this means $\rho_c = a_m$, as can be seen from Fig. 2. The size of the process zone and the microcrack density are limited by their elastic interaction to ≤ 0.5 /11,18,19/.

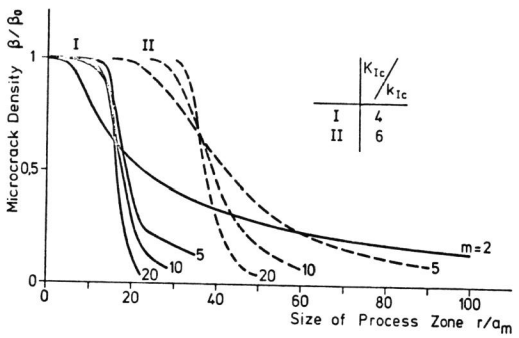

Fig. 1. Microcrack density of the microcracked region for different Weibull Moduli and stress intensity factors

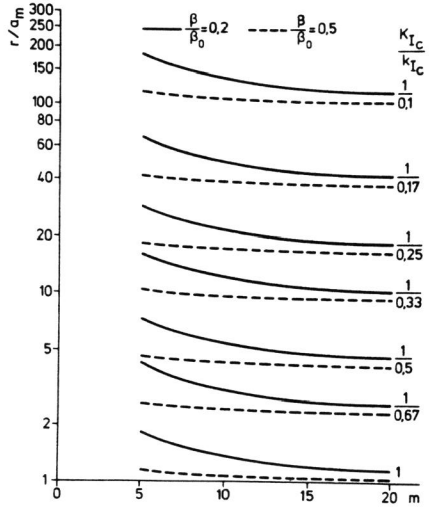

Fig. 2 Relative size of the microcracked region ahead of a macrocrack vs. Weibull modulus

The microcrack density ß for fine-grained Al_2O_3 materials is in the range of 0.2 to 0.5 /11/. Figure 2 shows for that range the size of the process zone for different values of the parameter $n(\sigma) = K_{Ic}/k_{Ic}$. B^+ is in the range of 0.8 to 3 for these microcrack densities.

As a consequence of that the local microscopic intergranular and transgranular

specific fracture energy γ_s has an essential influence on the size of the process zone. Little is known today about exact values of γ_s for specific ceramic materials. The Weibull-modulus m in the case of a large scattering of defects of a material, i.e. with small m-values, influences mainly the size of the process zone. In a first attempt for the physical and experimental interpretation of Fig. 1, values of 0.5 and 1 J/m^2 were used for γ_s. With the further assumption that the microcrack length a_m corresponds to about the average grain size $\bar{d}$, Fig. 3 shows a good agreement with our own experimental investigations of eight different Al_2O_3 ceramics, four each of qualities A and F, with specific chemical purity /3-7/.

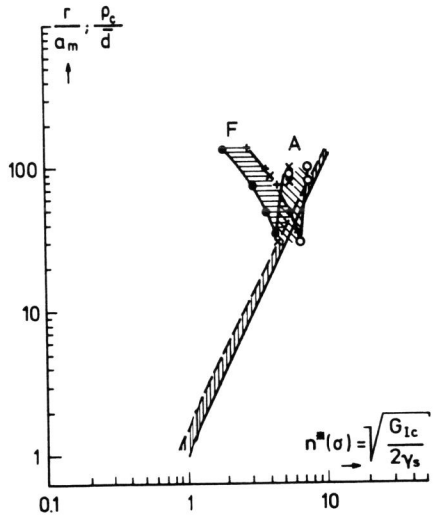

Fig. 3. Process zone vs. $n^*(\sigma) = \sqrt{G_{Ic}/2\gamma_s}$ for two aluminas

3. DISCUSSION

The characterization of ceramic materials by fracture-mechanic values is most usefully performed by the two-parameter expression of notch fracture mechanics made by Irwin /20/. His critical stress intensity factor K_{Ic} is given as

$$K_{Ic} = \frac{\sigma_{mc}}{2}\sqrt{\pi \rho_c} \qquad (10)$$

in the limit as the notch root radius tends toward ρ_c. σ_{mc} is the maximum notch fracture strength.

3.1 Material Parameters for Small-scale Microcrack Plasticity

Characterizing ceramic materials by means of stress intensity factors, the size of the process zone has a qualitatively comparable influence on the specimen dimensions, required to maintain a plane strain state, as is known from the interaction between the plastic zone and the specimen dimensions for metals. For Al_2O_3 ceramics concerning similar four-point-bent specimens it was found that the thickness B of these specimens with width W = B/2 has to fulfill the relation

$$B \geq 60 \left(\frac{K_{Ic}}{\sigma_{mc}}\right)^2 \qquad (11)$$

respectively, the notch root radius is given by

$$\rho \leq \rho_c = \frac{4}{\pi}\left(\frac{K_{Ic}}{\sigma_{mc}}\right)^2 \qquad (12)$$

The factor of 60 in eq. (11) characterizes an upper conservative limit. Misinterpretations of the influence of structure parameters on the stress intensity factor result, if these conditions are not fulfilled /6/.

Misinterpretations result, if due to too small specimens the formation of the process zone is not autonomous. The non-autonomy effects that the process zone cannot form itself in small specimens up to the critical size ρ_c, which holds for large specimens. The energy dissipation thus is smaller in small specimens than in large ones; this holds for a radius of curvatures $\rho < \rho_c$. For a radius of curvature $\rho > \rho_c$, however, K_I increases stronger for large specimens than for small ones.

The question arises concerning the physical reason for the lower K_I values of small specimens and notch root radii $\rho > \rho_c$ with regard to large specimens, i.e. the general increase of K_I values with the specimen volume. In earlier studies it was supposed that this geometry-dependence is caused by the expansion of regions plastified by microcracking in the specimens, that means, by the interaction of the process zone with geometric parameters. Theoretical estimations /2-6/ state that the notch fracture strength σ_{mc}, which in comparison to the Dugdale-Barenblatt model corresponds to a yield stress, decreases with decreasing Young's modulus E, i.e. $\sigma_{mc} = f(\sqrt{E})$. The Young's modulus E of an Al_2O_3 bent specimen is reduced, if the microcrack region involves wide areas of the ligament. σ_{mc} result experimentally according to eq. (10) from the slope of the $K_I = f(\sqrt{\rho})$ curve. For samples to which a plane strain state has to be associated (eq. (12)), $K_I = f(\sqrt{\rho})$ is a straight line, the prolongation of which crosses the origin. The microcrack region is then limited to the area of the process zone, corresponding to small scale yielding in metals. Then eq. (12) holds. The material behaves essentially linear-elastic.

The $K_I = f(\sqrt{\rho})$ curve, however, is bent concavely, and its slope decreases if the Young's modulus is decreased by microcracking. Large areas of the material in the region of the ligament are then plastified. The material behaves non-linear non-elastic. The deformation is associated to a plane stress state. These assumptions found preliminary confirmation on graphite materials, as is shown in the following section.

3.2 Material Parameters for Remote Microcrack Plasticity

Measurements of the $\sqrt{\rho}$-dependence of the stress intensity factor result $\sigma_{mc} \geq 10$ MPA for graphite ASR-2E. This value correlates with FEM calculations of Cords et al. /21/. It nearly corresponds to the tension strength of this material. By means of birefringent coatings, differences of the principal strains under load and undload condition were determined (Fig. 4). The size of the process zone, i.e. the area that has, because of microcrack plasticity, a low density compared to the surrounding material, is given by the "sharpest" notch bent radius with the highest possible notch stress, i.e. σ_{mc}. Because of the density decrease of the material in the process zone, the zone after unloading is under pressure stress. These

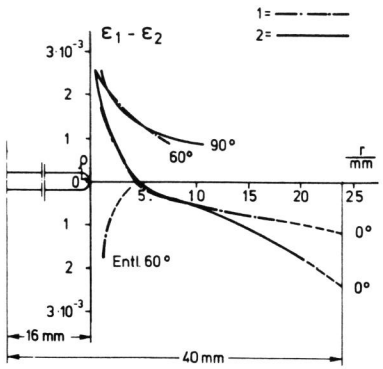

Fig. 4.
Distribution of the difference of principal strains ahead of a notch in the ligament field (0°) as well as the 60° and 90° lines of a four-point bent specimen of dimensions 20x40x250 mm during load by 392.4 N and after unloading (Entl.60°)

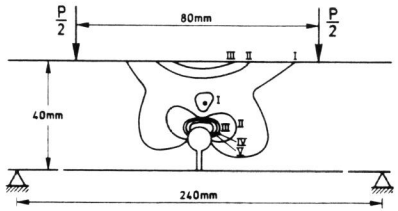

Fig. 5.
Photoelastic isochromatic pattern for the regions of microcracking in reactor graphite ASR-2E after "general microcracking" for K_I K_{Io} (beginning of stable crack growth) in a four-point bent specimen.
Curves of equal difference of principle strains:

I $\varepsilon_1 - \varepsilon_2 = 0.87 \cdot 10^{-3}$
II $\varepsilon_1 - \varepsilon_2 = 1.74 \cdot 10^{-3}$
III $\varepsilon_1 - \varepsilon_2 = 2.61 \cdot 10^{-3}$
IV $\varepsilon_1 - \varepsilon_2 = 3.48 \cdot 10^{-3}$
V $\varepsilon_1 - \varepsilon_2 = 4.35 \cdot 10^{-3}$

Material ASR-2E
Notch depth: 40 %
Notch root radius: specimen 1: $\rho \sim 0.2$ mm
specimen 2: $\rho \sim 4$ mm
Type of specimen: perpendicular to extrusion direction
Direction of crack propagation: parallel to extrusion direction
Bent stress
(total cross section) $\sigma_g = 2.94$ MPa
(net cross section) $\sigma_N^g = 8.17$ MPa
Stress intensity factor $K_1 = 0.878$ MPa $m^{1/2}$

pressure stresses arise since the density decrease after unloading cannot be cancelled completely; thus the microcracks are essentially irreversibly opened. The critical volume, which with stable crack-opening is subject to the notch crack stress σ_{mc}, is $\sim$ 1 cm /8/ for the largest investigated bent specimens. From the course of the line of same difference of the principal strains after unloading (Fig. 4), the value for the size of the process zone can be seen to be $\rho_c \approx 4$ mm for that reactor graphite for a crack running parallel to the extrusion direction. This value agrees reasonably with the measured values for σ_{mc} and K_{Io} according to eq. (10). The plastic failure of the material dominates compared to the elastic with increasing radius of curvature. A "plastic hinge", as shown in Fig. 5, is formed out. The crack release rate for $\rho > 1$ mm is independent of geometric parameters and can be regarded as a real material parameter.

The remote microcrack plasticity produces in the region of a ligament a reduced Young's modulus, E_{eff}, which because of $\sigma_{mc} = f(\sqrt{E})$ is the origin of the small notch strength. It has been shown that E_{eff} by means of measured values for the

Young's modulus in the as-received state E_o can be determined to

$$E_{eff} = \frac{E_o}{1 + J_{pl}/G_{Io}} \qquad (13)$$

For graphite ASR-2E, according to /22/, E_{eff} is in the range of 0.5 ... 0.8 E_o. σ_{mc} and E_{eff} involve a constitutive equation by which graphite structures can be calculated. These values, however, are dependent upon the load history.

3.3 Concluding Remarks

It is concluded according with preliminary experimental results that the above mentioned fracture mechanisms and rules are also valid for other fine and coarse grained ceramics like SiC or mullite refractories, respectively, with variations according to the specific microstructural parameters /24, 25/.

4. REFERENCES

/1/ Kusenko, V.S.: Concentration Criterion of Volume Fracture in Solids; in: Fracture Mechanics and Technology, Proc. Int. Conf. Hong Kong, 1977, eds. G.C. Sih, C.C. Chow, Vol. 1, 383-404.
/2/ Buresch, F.E.: A Model for the Fracture Strength of Ceramics and its Influence on Critical Fracture Stresses. Science of Ceramics, Vol. 7, published by Société Française de Céramique 1973, pp. 381-398.
/3/ Buresch, F.E.: About the process zone surrounding the crack tip in ceramics. Fracture 1977, Vol. 3, ICF4, Waterloo, Canada, June 1977, Ed. D.M.R. Taplin, Univ. of Waterloo Press, pp. 929-932.
/4/ Buresch, F.E.: Bewertung von Kennwerten der statischen Bruchmechanik. Ber. Dt. Keram. Ges. 54, 1977, 425-429.
/5/ Buresch, F.E.: A Structure Sensitive K_{Ic}-value and its dependence on grain size distribution, density and microcrack interaction, pp. 835-847, in: Fracture Mechanics of Ceramics, Vol. 4, 1978, pp. 835-847, eds. R.C. Bradt, D.P.H. Hasselman, F.F. Lange.
/6/ Buresch, F.E.: Fracture Toughness Testing of Alumina. Fracture Mechanics Applied to Brittle Materials ASTM STP 678, S.W. Freiman, Ed., ASTM, 1979, pp. 151-165.
/7/ Buresch, F.E.: Über den Einfluß von lokalen und integralen bruchmechanischen Kennwerten auf die Übertragbarkeit von Versagenskriterien; Berichte DVM Arbeitskreis Bruchvorgänge, 11. Sitzung, Stuttgart, 9.-11. Oktober 1979, 77-92.
/8/ Buresch, F.E., Müller, Th.: Einfluß von Kerb- und Probengeometrie auf das Verformungsverhalten sowie die bruchmechanischen Kennwerte eines Reaktorgraphits; Proc. Int. Conf. "Carbon 80", Baden-Baden, 30.6.-4.7.1980, to be published.
/9/ Freudenthal, A.M.: Statistical Approach to Brittle Fracture. Fracture III; Academic Press, New York 1968, 591-619.
/10/ Batdorf, S.B.: In Fracture Mechanics of Ceramics, Vol. 3, eds.: B.C. bradt, D.P.H. Hasselmann und F.E. Lange, Plenum Press, New York 1978, pp.1-30.
/11/ Buresch, F.E.: The Role of Microcracking on Fracture Toughness of Brittle Composites; Proc. Second European Colloquium on Fracture, ECF 2, "Fracture Mechanism and Mechanics", 9-11 Oct. 1978, Darmstadt, Germany, 256-268.
/12/ Blendell, J.E.; Coble, R.L., Charles, R.J.: On the Relaxation of Stresses Arising from Thermal Expansion Anisotropy during Cooling Polycrystalline Materials. In: Ceramic Microstructure "76", eds. Fulrath, Pask, pp.721-730.
/13/ Siebeneck, H.J.; Cleveland, J.J.; Hasselman, D.P.H.; Bradt, R.C.: Thermal Diffusivities of Microcracked Polycrystalline Ceramics. Pp. 753-762

/14/ Buresch, F.E.: Der Einfluß großer Eigenspannungen, bedingt durch die Bestrahlung mit schnellen Neutronen, auf die mechanischen Eigenschaften von Berylliumoxid. Science of Ceramics, Vol. 7, 1973, pp. 475.
/15/ Buresch, F.E.: unpublished work.
/16/ Broberg, K.B.: Crack Growth Criteria and Non-Linear Fracture Mechanics. Journal Mechanical Phys. Solids, Vol. 19, 1971, pp. 407-418.
/17/ A.G. Evans, A.H. Heuer, D.L. Porter; The Fracture Toughness of Ceramics, Fracture 1977, Vol. 1, ICF 4, Waterloo, Canada, June 1977, ed. D.M.R. Taplin, University of Waterloo Press Ontario, Canada, pp. 529-556.
/18/ Hoagland, R.G.; Embry, J.D.; Green, D.J.: On the Density of Microcracks formed during the Fracture of Ceramics. Scripta Metallurgica, Vol.9, 1975, pp. 907-909.
/19/ Delameter, W.R.; Herrmann, G.; Barnet, D.M.: Weaking of an Elastic Solid by a Rectangular Array of Cracks. Trans. ASME 1975, 74-80.
/20/ Irwin, G.R.: Fracture. In: S. Flügge: Handbuch der Physik, Bd. VI, S. 551-590, Berlin 1958.
/21/ Cords, H.; Djaloeis, A.; Kleist, G.; Öfinger, B.; Zimmermann, R.: Ein Beitrag zum Thema: Bruchkriterien über Graphit. JÜL-1355, Oktober 1976.
/22/ Buresch, F.E.: Mechanische Untersuchungen an Reaktorgraphit AS-II-500. IRW-IB-27/76.
/23/ Claussen, N.; Steeb, J., Pabst, R.F.: Effect of induced microcracking on the fracture toughness of ceramics. Journ. Amer. Ceram. Soc. 56, 1977, 559-562.
/24/ Rödig, M.; Buresch, F.E.: to be published.
/25/ Nickel, H.; Rödig, M.; Buresch, F.E.: Einfluß von Gitteranisotropie und Gefüge auf die Fertigkeit einiger keramischer Reaktorwerkstoffe, Science of Ceramics, Vol. 10. in press.